Correlated diffusion in quasi-low-dimensional systems

Raza A. Tahir-Kheli
Department of Physics, Temple University, Philadelphia, Pennsylvania 19122
(Received 27 October 1982)

The space- and time-dependent tracer occupancy correlation is solved for a general quasi-low-dimensional system with arbitrary concentration of hopping ions. Our theory is exact at both small and large ionic concentrations and gives reasonable results for all intermediate concentrations. Detailed numerical results for the diffusion correlation factor f^0, and the incoherent neutron scattering function $S(K,\omega)$, are provided for a variety of cases as the system changes gradually from three dimensional to one dimensional (1D), and vice versa. Similarly, the corresponding results associated with travel from two dimensions to 1D, and vice versa, are also recorded. Analytical expressions for f^0 as a function of the direction cosines of the wave vector are worked out for all limiting cases as the system approaches one, two, or three dimensionality. In particular, it is found that as one dimensionality is approached, the diffusion correlation factor approaches zero in proportion to the quantity $c^{-1}(J_\perp/J_{||})^{1/2}$.

I. INTRODUCTION

Stochastic hopping motion of classical particles, described in terms of simple rate equations, has been cited to be the central theme in a wide range of physical phenomena. Examples include ionic motion in superionic conductors,[1] diffusion of hydrogen in various metal hydrides,[2] and tracer atom diffusion in hot solids via the vacancy mechanism.[3] However, despite the stochasticity of the allowed hops, successive tracer-vacancy interchanges show correlations which arise because of the exclusion of double occupancy of any lattice site. These correlations were first noted by Bardeen and Herring,[4] and they affect both the short-range and the long-term characteristics of the hopping and extend over macroscopic space and time separations.[5,6] In three dimensions, correlations alter the small vacancy results quite substantially. Here, the diffusion coefficient is reduced[7] by as much as 35% (for the simple cubic lattice), and even more importantly, the rate of change of the tracer correlation function with vacancy diverges at the zone boundaries.[5]

The effects of the correlations are, however, much more substantial in lower dimensions. In two dimensions the reduction of the small vacancy tracer diffusion coefficient is more than 50% (for a square lattice) whereas in one dimension diffusion of a tracer completely ceases the instant the background stream contains any other particles.

These dramatic changes in the characteristics of ionic diffusion in one dimension (1D) were first described in an important paper by Richards.[8] The essentials of Richard's Monte Carlo results[8] were later corroborated by Fedders[9] (who used a diagrammatic summation procedure employing an improved version of his multiple-scattering approximation) and Alexander and Pincus[10] (who used simple arguments based on the coupling of single-particle motion to the density in 1D geometry).

Thus, reduction in dimensionality leads to fundamental and far-reaching changes in the details of ionic motion. Apart from the purely theoretical interest that such a happening generates, recent work on fast ion conductors has focused particular attention on the quasi-low-dimensionality (QLD) features of the ionic conductivity in these systems.[1] Prime examples of nearly 1D- and 2D-like ionic motion are provided by β-eucryptite[11] ($LiAlSiO_4$) and certain β-alumina.[12]

Experimental observation of the single-particle self-correlation function (note that the measurement of the self-diffusion coefficient D gives such a correlation function only for short wave vectors $\vec{K}$ and small frequencies ω) is generally limited to incoherent neutron scattering (INS) experiments.[2] Apart from their expense, neutron scattering experiments can only be performed in a few high-flux national facilities and are thus of limited accessibility. Nuclear magnetic resonance (NMR) techniques, on the other hand, are of much wider availability, but they generally measure two—specific-particle correlations (TSPC),[13] rather than the single—specific-particle correlations (SSPC) measured by INS. Un-

fortunately, however, the TSPC is much harder to evaluate than the SSPC.

Recent experimental developments, such as the magnetic "tagging" techniques,[14] have brought about a remarkable change in the state of affairs. Here the NMR linewidth data can be related to a frequency Fourier transform of the SSPC.[15–17] Accordingly, these developments have not only highlighted the relevance of the SSPC in general, they have also underscored the need for the SSPC in QLD systems[18] where relevant experiments have only recently been undertaken.[19,20]

In Sec. II, we present a formulation which distinguishes the hopping rate of the labeled ion (the "specific" particle) from that of the background ions. Moreover, we consider a spatially anisotropic lattice where the nearest-neighbor (NN) separation is different along the three Cartesian axes, being equal to a_x, a_y, a_z along directions x, y, z, respectively. Consistent with this anisotropy we assume different hopping rates along different axes, namely, J_x^0, J_y^0, and J_z^0 for the labeled ion, and J_x, J_y, and J_z for the background particles. However, we assume inversion symmetry in the lattice whereby

$$W^\sigma(\vec{i}-\vec{j})=W^\sigma(\vec{j}-\vec{i})=W_\alpha^\sigma, \text{ if } |\vec{i}-\vec{j}|=\delta_\alpha$$
$$=0, \text{ otherwise} \tag{1.1}$$

where, in the first equality, i and j, are nearest neighbors along axis α. Here $W_\alpha^\sigma=J_\alpha^0$ or J_α according to whether it relates to the labeled ion or the background particles and $\delta_\alpha=a_x,a_y,a_z$ when α equals x, y, or z, respectively. The advantage of such a formulation is that we can readily change the dimensionality from 3D to anisotropic 2D (by putting $J_z^0=J_z=0$, say) and on to 1D in a fairly general fashion. The mean-field approximation (MFA), often times called the random-walk solution for the SSPC is presented in this section.

In Sec. III the second-order solution (SOS) is worked out. The result is given in terms of six coupled linear equations, for the six components of the mass operator referring to the six NN separations $\vec{\delta}_\alpha$. While the various coefficients occurring in these equations require tedious numerical computations for general frequencies ω and wave vectors $\vec{K}$ in the small-frequency limit $\omega \ll \sum_\alpha J_\alpha^0$ when the wave vectors are also very small, i.e., $\sum_\alpha K_\alpha^2 a_\alpha^2 \ll 1$, analytical methods can be used to recast these equations into a particularly simple form. This is, of course, the well-known diffusive limit.

Detailed numerical results for general frequencies and wave vectors are presented and discussed in the concluding Sec. IV. However, for the sake of brevity, computations are presented only for the case of cylindrical symmetry.

II. FORMULATION

We begin by introducing the rate equation that is assumed to be satisfied by the stochastic occupancy variables of the labeled atom, $p_i(t)$, and that of the background particles, $n_i(t)$. As usual, an occupancy variable is unity if the site i at time t is occupied by the specific atom, i.e., $p_i(t)=1$, or any of the background atoms, i.e., $n_i(t)=1$. Otherwise, the relevant occupancy variable is zero. We can write the rate equation as

$$\frac{d\sigma_i}{dt}=-\sum_j W^\sigma(\vec{i}-\vec{j})(\sigma_i V_j-\sigma_j V_i) , \tag{2.1}$$

where $\sigma_i \equiv p_i$ or n_i according to whether $W^\sigma(\vec{i}-\vec{j})=J^0(\vec{i}-\vec{j})$ or $J(\vec{i}-\vec{j})$, and V_j is the occupancy variable specifying a vacancy at site i, i.e.,

$$V_i=1-p_i-n_i . \tag{2.2}$$

This model assumes that there is only a single labeled ion, that other than the point hard-core repulsion there are no interparticle interactions, that the hopping transit time is short, the concentration of hopping particles is c, and that the concentration of vacancies is v, i.e.,

$$\langle n_i \rangle = c, \quad \langle V_i \rangle = v = 1-c . \tag{2.3}$$

(Note that, compared with unity, terms of order $1/N$ will be ignored where N is the number of sites in the lattice.)

In order to calculate the SSPC, it is convenient to work with the single–specific-particle (SSP) Green's function

$$G_{gg'}(t)=-2\pi i\Theta(t)\langle p_g(t)p_{g'}(0)\rangle \tag{2.4}$$

and its frequency Fourier transform

$$G_{gg'}\equiv\langle\langle p_g;p_{g'}\rangle\rangle$$
$$=\frac{1}{2\pi}\int_{-\infty}^{+\infty} dt\, G_{gg'}(t)\exp(i\omega t) . \tag{2.5}$$

In (2.4), $\Theta(t)$ represents the Heaviside unit step function and the single angular brackets signify an ensemble coverage.

The rate equation (2.1) leads to the following equation of motion (EM) for the SSP Green's function G, i.e.,

$$\omega G_{gg'}=\delta_{gg'}-iv\sum_j J^0(\vec{g}-\vec{j})(G_{gg'}-G_{jg'})$$
$$+i\sum_j J^0(\vec{g}-\vec{j})(\Gamma_{gj;g'}-\Gamma_{jg;g'}) , \tag{2.6}$$

where Γ is a second-order fluctuation (SOF) Green's function defined as

$$\Gamma_{lj;g'}=\langle\langle p_l u_j;p_{g'}\rangle\rangle\ , \tag{2.7a}$$

$$u_j=n_j-c,\ \ \langle u_j\rangle=0\ . \tag{2.7b}$$

Within the simple MFA, the SOF is ignored as being "small" and thus we get

$$G_K^{\mathrm{MFA}}=(\omega+iv\omega_K^0)^{-1}\ , \tag{2.8}$$

$$\omega_K^0=2\sum_\alpha J_\alpha^0[1-\cos(K_\alpha a_\alpha)]\ . \tag{2.9}$$

For $k^2\ll 1$, the spectral line shape is entirely diffusive, i.e.,

$$G_K^{\mathrm{MFA}}=(\omega+ivD_0k^2)^{-1}\ , \tag{2.10a}$$

where $\vec{K}=k(\beta_x,\beta_y,\beta_z)$, β_α being the direction cosines of the wave vector $\vec{K}$ and

$$D_0=\sum_\alpha J_\alpha^0\beta_\alpha^2 a_\alpha^2\ . \tag{2.10b}$$

The self-diffusion coefficient of the ion, vD_0, is thus a function of the direction in which the diffusion is taking place.

For the isotropic lattice, the foregoing result is known to be in error in both 3D and 2D, by approximately 35% and 53%, respectively. In 1D it is even wrong qualitatively. Here the diffusion coefficient is known to be vanishing[8] as long as $c\neq 0$.

A feel for the relative accuracy of the MFA can be had from the following simple argument. On the right-hand side (rhs) of Eq. (2.6) the neglect of the terms proportional to Γ, in comparison with those proportional to G, will affect the mass operator for G_K—which in the MFA is proportional to $\omega_K^0 v$—by terms proportional to $\omega_K^0(\Gamma_K/G_K)$. The ratio of these Green's functions, however, should be of the order of the variance of u_j, i.e., of order

$$\langle u_j^2\rangle\simeq cv\ . \tag{2.11}$$

Thus the mass operator, for instance, $\Sigma(\vec{K},\omega)$, can be expected to be of the form

$$\Sigma(\vec{K},\omega)=v\omega_K^0+\cdots \simeq v\omega_K^0+O(cv)\omega_K^0\ , \tag{2.12}$$

where the ellipsis represents fluctuation terms. The relative important of the fluctuation terms (as compared to those that are retained in the MFA) is thus of order c. For small enough concentration, i.e., $c\ll 1$, fluctuations from the MFA should, therefore, be small. This, however, is true only as long as the connectivity of the lattice is such that the MFA itself is not qualitatively in error, for if this should be the case, it makes hardly any sense to look for small fluctuations from the MFA. In this regard we remind ourselves of the well-known property of the MFA, namely, that it becomes asymptotically exact as the effective number of neighbors becomes large. From the work of Richards[8] and others,[9,10] it appears that the MFA breaks down qualitatively only when the motion is rigorously restricted to one dimension. Thus, in 1D our simple estimate for the size of fluctuations from the MFA is valid in only the trivial limit $c=0$. As soon as $c\neq 0$, we can expect the neglected terms to be of the same order as the MFA itself.

III. FLUCTUATIONS FROM THE MEAN FIELD

In view of the inadequacy of the MFA, an improved SOS is essential, especially in QLD systems. To this end we study next the EM of the Green's function Γ. We get

$$\begin{aligned}-i\omega\Gamma_{lj;g'}=&c[J^0(\vec{l}-\vec{j})v+J(\vec{l}-\vec{j})+(i\omega-\tau^0 v-\tau)\delta_{lj}]G_{lg'}\\&+\Gamma_{lj;g'}[(1-2c)J^0(\vec{l}-\vec{j})+J(\vec{l}-\vec{j})-\tau^0 v-\tau]+cJ^0(\vec{l}-\vec{j})\Gamma_{jl;g'}\\&+(1-\delta_{lj})\sum_i[vJ^0(\vec{l}-\vec{i})\Gamma_{ij;g'}+J(\vec{j}-\vec{i})\Gamma_{li;g'}]+\mathscr{R}(l,j,g')\ .\end{aligned} \tag{3.1}$$

This equation is exact. The new notation introduced is as follows:

$$\mathscr{R}(l,j,g')=\sum_i J^0(\vec{l}-\vec{i})(1-\delta_{lj})(1-\delta_{ij})\times\langle\langle(p_l u_i-p_i u_l)u_j;p_{g'}\rangle\rangle\ , \tag{3.2}$$

$$\tau^0=2(J_x^0+J_y^0+J_z^0),\ \ \tau=2(J_x+J_y+J_z)\ . \tag{3.3}$$

The third-order term (TOT), denoted by $\mathscr{R}$, involves at least two fluctuation fields and refers to three different particles at positions l,i,j which are, of course, all different. Moreover, much like the second-order terms on the rhs of (2.6), the third-order term also involves a mutually subtractive structure of the form $(p_l u_i-p_i u_l)$ referring to neighboring sites i and l. Accordingly, we anticipate that relative to the terms being retained, neglecting the TOT would cause errors in the mass operator of the order of

$$v^{-1}\langle u_i^2 u_j^2\rangle_{i\neq j}\simeq O(c^2 v)\ .$$

This represents a considerable improvement because c^2v is small in both the $c \ll 1$ and $v \ll 1$ limits. Also, for the worst case, $c=v=\frac{1}{2}$, it is $\frac{1}{8}$. Finally, for small c, the omitted terms are now of order c^2, rather than c, as was previously the case. Accordingly, we expect that, even in 1D, the predictions of the second-order theory would be qualitatively correct. A detailed examination of this point is best deferred to Sec. IV.

Neglecting $\mathscr{R}$, an exact solution of Eqs. (2.6) and (3.1) can be achieved. In order to carry this out we use inverse lattice Fourier transformation. First, it is convenient to recast (2.6) as follows:

$$[\omega+i\Sigma(\vec{K},\omega)]G_K=1 , \tag{3.4}$$

where

$$G_{gg'}=(1/N)\sum_{\vec{K}} G_K \exp[i\vec{K}\cdot(\vec{g}-\vec{g}')] , \tag{3.5a}$$

$$\Sigma(\vec{K},\omega)=v\omega_K^0+\sum_{\vec{\delta}} J^0(\vec{\delta})\rho(\vec{\delta})[\exp(i\vec{K}\cdot\vec{\delta})-1] . \tag{3.5b}$$

The sum $\sum_{\vec{\delta}}$ spans over six NN vectors, $\pm\vec{\delta}_x$, $\pm\vec{\delta}_y$, and $\pm\vec{\delta}_z$, and

$$\rho(\vec{\delta})=\frac{1}{N}\sum_{\lambda}\Gamma_{K-\lambda,\lambda}\exp(-i\vec{\lambda}\cdot\vec{\delta})/G_K , \tag{3.5c}$$

$$\Gamma_{lj;g'}=\left[\frac{1}{N}\right]^2\sum_{\lambda_1}\sum_{\lambda_2}\Gamma_{\lambda_1,\lambda_2}\exp[i\vec{K}_1\cdot(\vec{l}-\vec{g}')+i\vec{K}_2\cdot(\vec{j}-\vec{g}')] . \tag{3.5d}$$

Next, we examine (3.1). We employ the Fourier transformation (3.5d), and regroup the various terms in Eq. (3.1). This leads to the following relationship for the quantities $\rho(\vec{\delta})$:

$$\rho(\vec{\delta})=\Phi(\vec{\delta})+\sum_{\vec{\delta}'}\rho(\vec{\delta}')\{J^0(\vec{\delta}')\exp(i\vec{K}\cdot\vec{\delta}')[cP(\vec{\delta}+\vec{\delta}')-vP(\vec{\delta}')] +[J(\vec{\delta}')+J^0(\vec{\delta}')(1-2c)]P(\vec{\delta}-\vec{\delta}')-J(\vec{\delta}')P(\delta)\} , \tag{3.6}$$

where

$$P(\vec{r})=\frac{1}{N}\sum_{\lambda}\exp(i\vec{\lambda}\cdot\vec{r})/E(\lambda) , \tag{3.7a}$$

$$\Phi(\vec{\delta})=icv\frac{1}{N}\sum_{\lambda}\exp(i\vec{\lambda}\cdot\vec{\delta})(\omega^0_{K+\lambda}-\omega^0_{\lambda})/E(\lambda) , \tag{3.7b}$$

$$E(\lambda)=\omega+i(\omega_\lambda+v\omega^0_{K+\lambda}) , \tag{3.7c}$$

$$\omega_\lambda=2\sum_{\alpha}J_\alpha[1-\cos(\lambda_\alpha a_\alpha)] . \tag{3.7d}$$

The mass operator is thus seen to depend on six quantities $\rho(\vec{\delta})$ which, in turn, are determined from Eq. (3.6), the latter being a set of six coupled linear equations. For general $\vec{K}$ and ω, the evaluation of parameters $\Phi(\vec{\delta})$ and $P(\vec{r})$ requires cumbersome numerical computation. However, as mentioned in the Introduction, in the long-wavelength small-ω limit the mass operator can be cast into a particularly simple form by using analytical models. This involves tedious but elementary algebra and the result is found to be the following:

$$vD_0f^0k^2=\lim_{Dk^2/\omega\to 0}\lim_{\omega/\tau_0\to 0}\Sigma(\vec{K},\omega) , \tag{3.8}$$

where f^0 is the so-called correlation factor[3] and, unlike in isotropic lattices, is now a function of the direction of diffusion, i.e.,

$$f^0\equiv f^0(\beta_x,\beta_y,\beta_z) =1+(2c/D_0)\sum_{\alpha}(J^0_\alpha)^2T_\alpha(\beta_\alpha a_\alpha)^2/(1+\nu_\alpha T_\alpha) . \tag{3.9}$$

Here D_0 is as in (2.10b) and

$$\nu_\alpha=J_\alpha+J^0_\alpha(1-3c) , \tag{3.10a}$$

$$T_\alpha=\frac{1}{N}\sum_{\lambda}[\cos(2\lambda_\alpha a_\alpha)-1]/Y(\lambda) , \tag{3.10b}$$

$$Y(\lambda)=2\sum_{\alpha}(J_\alpha+vJ^0_\alpha)[1-\cos(\lambda_\alpha a_\alpha)] . \tag{3.10c}$$

It is clear that the inverse lattice sums T_α are a generalized version of the well-known quantity $\langle\cos\theta\rangle$ that arises in isotropic lattices.[3] For instance, in the limit of isotropy, i.e.,

$$J^0_\alpha\equiv J^0,\ J_\alpha=J,\ a_\alpha=a \text{ for } \alpha=x,y,z \tag{3.11}$$

$$T_\alpha=(J+vJ^0)^{-1}\langle\cos\theta\rangle . \tag{3.12}$$

Now, using the fact that

$$\sum_{\alpha}(\beta_\alpha)^2=1 , \tag{3.13}$$

we find f^0 independent of the direction cosines β_α, i.e.,

$$f^0=\left[1-\frac{2J^0c\langle\cos\theta\rangle}{(J+vJ^0)(1+\langle\cos\theta\rangle)}\right]^{-1}. \tag{3.14}$$

This is, of course, the result obtained for isotropic lattices.[7]

IV. RESULTS

In view of the proliferation of parameters in the general formulation presented in the preceding sections, and the fact that all the relevant computations are straightforward to carry out should the need arise, in what follows we limit ourselves to a simple subset of parameters. This subset is appropriate to the most familiar QLD systems where the labeled ion is similar to those hopping in the background. More specifically, we restrict all future discussion to the following model:

$$J_\alpha^0=J_\alpha\ , \tag{4.1}$$

$$J_x=J_y=J_\perp,\ \ J_z=J_{||}\ , \tag{4.2}$$

$$a_x=a_y=a_\perp,\ \ a_z=a_{||}\ . \tag{4.3}$$

Thus the only relevant parameter specifying the QLD features of the problem is the ratio

$$\eta=J_\perp/J_{||}\ , \tag{4.4}$$

that is, as long as the interatomic separations, $a_\perp$ and $a_{||}$, are included as the relevant normalization factors for the inverse lattice wave vectors. Accordingly, henceforth, we shall use the notation

$$K_xa_\perp=k_x,\ \ K_ya_\perp=k_y,\ \ K_za_{||}=k_z\ . \tag{4.5}$$

The dimensionless wave vectors k_α will thus form a simple cubiclike Brillouin zone, $-\pi\le k_\alpha\le\pi$. As η varies from 0 to 1, the effective dimensionality of our physical system ranges from 1D (the uncoupled linear chains extend along the z direction) to 3D. Similarly, the system varies from 3D to 2D as η^{-1} ranges between 1 and 0. Here the relevant 2D system consists of uncoupled quadratic layers parallel to the x-y plane. In this format, the directional dependence of $F(\vec{\mathbf{K}},\omega)$ is reduced to two effective direction cosines $\beta_\perp$ and $\beta_{||}$, where

$$\beta_\perp=(\beta_x^2+\beta_y^2)^{1/2},\ \ \beta_{||}=\beta_z\ . \tag{4.6}$$

Accordingly, for brevity as well as convenience, vector notation will be abbreviated along the following lines:

$$\vec{\mathbf{K}}=(k_\perp;k_{||}),\ \ f^0(\beta_x,\beta_y,\beta_z)=f^0(\beta_\perp;\beta_{||})\ . \tag{4.7}$$

Let us first examine the behavior of $f^0(0;1)$. This refers to diffusion which is purely along the z axis. From Eq. (3.9) we get

$$f^0(0;1)=[1+(1+v)T_{||}]/[1+(3v-1)T_{||}]\ , \tag{4.8}$$

where

$$T_{||}=\frac{1}{2N}\sum_\lambda\frac{(c_{2z}-1)}{(1+v)[1-c_z+\eta(2-c_x-c_y)]} \tag{4.9}$$

and

$$c_{n\alpha}\equiv\cos(n\lambda_\alpha a_\alpha)\ . \tag{4.10}$$

We notice that the correlation factor depends only on the ratio η and not on the individual values of the longitudinal and transverse hopping rates.

In the 1D limit, $T_{||}$ is especially simple, i.e.,

$$\lim_{\eta=0}T_{||}=-(1+v)^{-1} \tag{4.11}$$

and hence for $c\neq0$,

$$f^0(0;1)=0\ . \tag{4.12}$$

This is well known but nevertheless important because it demonstrates that the present formulation is in accord with the absence of self-diffusion in 1D.[8] However, for finite η, self-diffusion does occur and it is a simple matter to estimate the corresponding integral $T_{||}$ when η is small compared to 1. We get

$$T_{||}\underset{\eta\ll1}{\sim}(1+v)^{-1}[-1+2h_0\eta^{1/2}+O(\eta)]\ , \tag{4.13a}$$

where

$$h_0\sim(2\pi)^{-2}\int\int_{-\pi}^{+\pi}dx\,dy[1-(\cos x+\cos y)/2]^{1/2}\ .$$

A word of caution is in order regarding Eq. (4.13a) in particular, and, in general, all the subsequent equations that relate to the limit in which one dimensionality is approached. Here, the tracer diffusion is drastically reduced due to correlations. It is, therefore, necessary to take account of this reduction in the second-order equation of motion (3.1), or equivalently, its solution given in (3.6). This is a lengthy procedure and will be described in detail elsewhere. For the present purposes, it suffices to say that the net effect of this renormalization is quite small. It affects only the concentration dependence of the multiplying factor to the $\eta^{1/2}$ term in Eq. (4.13a), changing it from $(1+v)$ to $[1+O(v\eta^{1/2})]$, which, in turn, approaches unity as $\eta\to0$. No corresponding role is played by such renormalization in the opposite limit, i.e., $\eta\to\infty$,

where we estimate

$$T_{\|}=\lim_{\eta^{-1}\to 0} -(1+v)^{-1}\frac{h_1}{2}(\eta^{-1}\ln\eta)-O(\eta^{-1}) , \tag{4.13b}$$

where $h_1\sim 2/\pi^2$. Hence we get

$$f^0(0;1)=\lim_{\eta^{-1}\to 0} 1-\frac{h_1 c(\eta^{-2}\ln\eta)}{(1+v)}-O(c\eta^{-1}) , \tag{4.14a}$$

$$f^0(0;1)=\lim_{\eta\to 0} h_0(\eta c^{-1})^{1/2}+O(\eta c^{-2}) . \tag{4.14b}$$

For arbitrary concentration c, as $\eta^{-1}\to 0$, the diffusion along the chains becomes random-walk-like. This is not surprising since it is trivially known that as long as c is rigorously zero (i.e., the lattice is completely empty except for the labeled atom), f^0 is 1. On the other hand, in the opposite limit, i.e., $\eta c^{-2}\ll 1$ [see Eq. (4.14b)], the above result is nontrivial both for small η and small c. Indeed, it demonstrates that for finite c, the rate of increase of diffusion along the chains is divergent for $\eta\to 0$. A hint of just such a happenstance has recently been noted in some very preliminary Monte Carlo work being done at Jülich.[21]

To contrast the above behavior of diffusion along the chains with that of diffusion confined to the transverse x-y planes, let us examine the correlation parameter $f^0(1;0)$. From Eqs. (3.9), (3.10), (4.3), and (4.4) we get

$$f^0(1;0)=1+2cT_\perp/[1+(3v-1)T_\perp] , \tag{4.15}$$

where

$$T_\perp=\left[\frac{\eta}{2(1+v)}\right]\frac{1}{N}\sum_\lambda \frac{(c_{2x}-1)}{1-c_z+\eta(2-c_x-c_y)} . \tag{4.16}$$

For $\eta\ll 1$, we can again estimate the sum. To the dominant order we get

$$T_\perp \underset{\eta\ll 1}{\sim} -h_2\eta^{-1/2}/[2(1+v)]+O(1) , \tag{4.17}$$

where h_2 is approximately given by the following 2D sum:

$$h_2\approx(\sqrt{2}\pi^2)^{-1}\times\int_0^\pi\int_0^\pi dx\,dy(1-\cos 2x)/(2-\cos x-\cos y)^{1/2} .$$

Hence

$$f^0(1;0) \underset{\eta\ll 1}{\sim} 1-ch_2\eta^{1/2}/(1+v)-O(\eta) . \tag{4.18}$$

The significance of this result should not be missed. It expresses the fact that when intraplanar hopping is much slower than the intrachain hopping, the ionic diffusion within the planes is essentially uncorrelated, i.e., it is random-walk-like and, accordingly, $f^0(1;0)$ is nearly unity. In the opposite limit, i.e., when $\eta\gg 1$ and the diffusion is largely restricted to the planes, we already know from (4.14a) that diffusion along the chains is weak but uncorrelated. Thus, despite its different appearance, Eq. (4.18) is very similar in its physical content to the result given in (4.14a).

Finally, we estimate $T_\perp$ for the opposite limit, i.e., when $\eta^{-1}\ll 1$. We write

$$T_\perp=(1+v)^{-1}\frac{1}{N}\sum_\lambda \frac{(c_{2x}-1)}{4-2c_x-2c_y+2\eta^{-1}(1-c_z)} \tag{4.19}$$

as $\eta^{-1}\to 0$, this gives

$$T_\perp=(1+v)^{-1}[\langle\cos\theta\rangle_{2D}+h_3(\eta^{-1}\ln\eta)] , \tag{4.20}$$

where

$$\langle\cos\theta\rangle_{2D}=(2N)^{-1}\sum_\lambda (c_{2x}-1)/(2-c_x-c_y) . \tag{4.21}$$

Thus for $\eta\gg 1$

$$f^0(1;0)=f^0_{2D}+\frac{2ch_3(1+v)}{[1+v+(3v-1)\langle\cos\theta\rangle_{2D}]^2}\times(\eta^{-1}\ln\eta)+O(\eta^{-1}) . \tag{4.22}$$

Here h_3 is approximately equal to h_1 and f^0_{2D} is the correlation factor for isotropic diffusion in 2D, i.e.,

$$f^0_{2D}=\left[1-\frac{2c\langle\cos\theta\rangle_{2D}}{(1+v)(1+\langle\cos\theta\rangle_{2D})}\right]^{-1} . \tag{4.23}$$

We have numerically estimated the parameter free sum $\langle\cos\theta\rangle_{2D}$ given in (4.21) and find it to be $\approx -0.3634\pm 0.000\,05$.

The physical consequences of Eq. (4.22) are the following. If intrachain hopping rates are small compared to the intraplanar hopping rates, the diffusion characteristics of the ion within the planes are only weakly affected by the interplanar hopping. The motion thus displays the correlation characteristic of the purely 2D case. Note also that the rate of increase of $f^0(1;0)$, with η^{-1}, is logarithmic in the limit where η^{-1} is small. This is in striking contrast with the corresponding, nearly 1D result for $\eta\to 0$ given in (4.14b). Thus the presence of even a single additional linear chain, with slow interchain hopping, would increase diffusion along the

original chain precipitously. No such dramatic effect should be noticeable when diffusion is being monitored in a 2D sheet and an additional sheet with weak interplanar hopping is added.

So far in this section we have examined only the diffusive limit, namely, the long-wavelength small-frequency limit. Most experiments, however, detect the SSPC at general wave vectors and frequencies. Accordingly, it is convenient to introduce the generalized correlation factor $F(\vec{K},\omega)$ as follows:

$$\Sigma(\vec{K},\omega)=v\omega_K^0 F(\vec{K},\omega)\ . \tag{4.24}$$

On comparison with (3.8), it is readily confirmed that the two correlation factors are related, i.e.,

$$\lim_{D_0k^2/\omega\to 0}\ \lim_{\omega/\tau_0\to 0} F(\vec{K},\omega)=f^0(\beta_x,\beta_y,\beta_z)\ . \tag{4.25}$$

However, unlike f^0, for general $\vec{K}$ and ω only numerical solution is possible for $F(\vec{K},\omega)$. Because the correlation is generally most significant for small frequencies and low vacancy concentration, in Fig. 1 we show $F(\vec{K},0)$ for the limit $v\to 0$. Parameters $f^0(0;1)$ and $f^0(1;0)$ are given as solid lines labeled a and b, respectively. The corresponding dashed curves show $F(\vec{K},0)$ with $(K_\alpha a_\alpha)=(0,0,\pi)$ and $(\pi,\pi,0)$, respectively. For the sake of generality we have also given the correlation factor $F(\vec{K},0)$ at the zone edge along the cube diagonal, i.e., $(K_\alpha a_\alpha)=(\pi,\pi,\pi)$—this is shown as the dashed curve labeled c. The solid curve marked c refers to $f^0(1/\sqrt{3},1/\sqrt{3},1/\sqrt{3})$. The nice feature of such a plot is that it spans two-thirds of the relevant dimensionality space, namely, 3D↔1D as well as 3D↔2D. The numerically computed results seem to corroborate the analytical ones given above although the detail of the singularity of the slopes near $\eta\to 0$ and $\eta^{-1}\to 0$ is hard to determine accurately. Another important aspect of these results is that motion along the [111] direction is seen to considerably accentuate the slopes near the 2D limit, i.e., the correlation factors for $\eta^{-1}\to 0$ for direction along the [111] diagonal rise more steeply than those referring to the purely planar diffusive motion along the [110] direction.

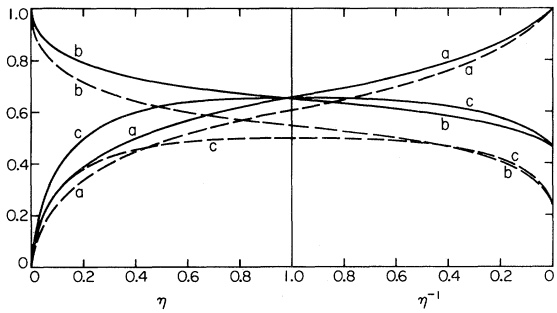

FIG. 1. For the limit $v\to 0$, the diffusion correlation factor f^0 (shown as full curves) as well as the generalized correlation factor for zero frequency $F(\vec{K},0)$ (dashed curves) are plotted as a function of η. Curves a, b, and c refer to motion along the longitudinal linear chains, i.e., parallel to [001]; within the x-y planes, i.e., parallel to [110]; and along the cube diagonal [111], respectively. For the dashed curves a, b, and c, the wave vector is at the zone edge; i.e., for these curves $(K_xa_x,K_ya_y,K_za_z)=(0,0,\pi)$, $(\pi,\pi,0)$, and (π,π,π), respectively.

Given the interest in the rapid increase in intrachain diffusion, when a small number of additional chains with weak interchain hopping are introduced,[21] it is essential that the line of investigation presented above be fully completed. This means that in addition to the 1D↔3D↔2D analysis, we must also examine the 1D↔2D characteristics of the problem. To this end, we consider a system with a quadratic lattice in the x-y plane, with NN separations a_x and a_y and hopping sites J_x and J_y. (For simplicity, we continue to assume $J_\alpha^0=J_\alpha$.) Let us call the ratio $J_x/J_y=\mu$. Then the relevant expression for such a correlation parameter $f^0(\beta_x,\beta_y)$ can be readily found from the general three-dimensional result given in Eq. (3.9). Accordingly, we can write

$$f^0(0;1)=[1+(1+v)T_y]/[1+(3v-1)T_y]\ , \tag{4.26}$$

$$T_y=[2(1+v)]^{-1}\times\frac{1}{N}\sum_\lambda (c_{2y}-1)/[1-c_y+\mu(1-c_x)]\ . \tag{4.27}$$

For $\mu\ll 1$, we get

$$T_y=(1+v)^{-1}[-1+2h_4\mu^{1/2}+O(\mu)]\ , \tag{4.28}$$

where $h_4\sim 2/\pi$ and hence the renormalized result is the following:

$$\lim_{\mu\to 0} f^0(0;1)=h_4(\mu c^{-2})^{1/2}+O(\mu c^{-2}) \tag{4.29}$$

[compare Eq. (4.14b)]. It is interesting to note that h_4 is roughly two-thirds of h_0. Thus both the structure of the singularity as well as its prefactor are essentially the same whether the passage is 1D→3D or 1D→2D.

For $f^0(1;0)$ similar analysis gives

$$f^0(1;0)=1-ch_5(1+v)^{-1}\mu^{1/2}-O(\mu)\ , \tag{4.30}$$

where $h_5\sim 8/3\pi$. Again, in going from 1D→2D the initial behavior is very similar to the correspond-

ing one found for the travel 1D→3D [cf. Eq. (4.18)].

Such a symmetry is, however, broken when we consider the travel from 2D→1D. Here, in contrast to Eq. (4.22), we get

$$f^0(0;1)=\lim_{\epsilon\to 0} f^0_{2D}+M_1\epsilon\ , \tag{4.31a}$$

$$f^0(0;1)=\lim_{\epsilon\to 0} f^0_{2D}-M_2\epsilon\ , \tag{4.31b}$$

where M_1 and M_2 are finite constants dependent on concentration c and ϵ is a measure of the departure from 2D in the direction of 1D, i.e.,

$$\epsilon=|1-\mu|\ . \tag{4.32}$$

For $v\to 0$, $M_1=M_2\cong 0.147$; compare curves 1 and 4 in Fig. 2. [Note that Eqs. (4.31) cannot usefully be contrasted with Eq. (4.14a) because the latter relates to an altogether different physical situation. Indeed, it is more reasonable to compare the content of Eq. (4.14a) with that of (4.30).]

To supplement the analytical results, which for the sake of convenience have been set out in the form of tables (see Tables I and II), in Fig. 2 we present the 1D↔2D version of the plot given in Fig. 1. Here the $v\to 0$ results for $f^0(0,1)$, $f^0(1;0)$, and $f^0(1;1)$ are given as a function of μ. Again, for useful comparison, results for $F(\vec{K},0)$ with

TABLE I. For the 3D↔1D traversals, the diffusion correlation factor $f^0\equiv f^0(\beta_x,\beta_y,\beta_z)$, corresponding to an infinitesimal wave vector $\vec{K}$ with direction cosines $(\beta_x,\beta_y,\beta_z)$, is presented as a function of the ratio $J_\perp/J_{||}=\eta$. Here, for convenience, we have restricted ourselves to the case where the tracer hopping rates J^0_α are equal to those of the background particles J_α and have further assumed the x-y symmetry, i.e., $J^0_x=J^0_y=J_x=J_y=J_\perp$ and $J^0_z=J_z=J_{||}$. Moreover, for brevity, we have used the notation $f^0(\beta_x,\beta_y,0)=f^0(1;0)$ and $f^0(0,0,1)=f^0(0;1)$. The quantity f^0_{2D} is defined to be $(1+\langle\cos\theta\rangle_{2D})/(1-\langle\cos\theta\rangle_{2D})$ where the quantity $\langle\cos\theta\rangle_{2D}$ is equal to the 2D integral specified in Eq. (4.21). [Note: for relating of $F(\vec{K},\omega)$ to $f^0(\beta_x,\beta_y,\beta_z)$, see Eq. (4.25)].

$\lim_{\eta\to 0} f^0(0;1)=h_0(\eta c^{-2})^{1/2}$
$\lim_{\eta\to\infty} f^0(0;1)=1-h_1\left[\frac{c}{1+v}\right]\eta^{-1}\ln\eta$
$\lim_{\eta\to 0} f^0(1;0)=1-h_2\left[\frac{c}{1+v}\right]\eta^{1/2}$
$\lim_{\eta\to\infty} f^0(1;0)=f^0_{2D}+\frac{2h_3c(1+v)}{1+v+(2-3c)\langle\cos\theta\rangle_{2D}}(\eta^{-1}\ln\eta)$

TABLE II. For the 2D↔1D traversals, the diffusion correlation factor $f^0(\beta_x,\beta_y)$, corresponding to a 2D infinitesimal wave vector $\vec{K}$ with direction cosines (β_x,β_y), is presented as a function of the ratio $J_x/J_y=\mu$. Again, for simplicity, in this analytical work we have confined ourselves to the case where $J^0_\alpha=J_\alpha$. When approaching the 2D limit, it is convenient to work with the quantity $\epsilon=|1-\mu|$.

$\lim_{\mu\to 0} f^0(0;1)=h_4(\mu c^{-2})^{1/2}$
$\lim_{\mu\to 0} f^0(1;0)=1-\left[\frac{c}{1+v}\right]h_5\mu^{1/2}$
$\lim_{\epsilon\to 0} f^0(0;1)=f^0_{2D}+M_1\epsilon$
$\lim_{\epsilon\to 0} f^0(1;0)=f^0_{2D}-M_2\epsilon$
$M_1=M_2\simeq 0.147$

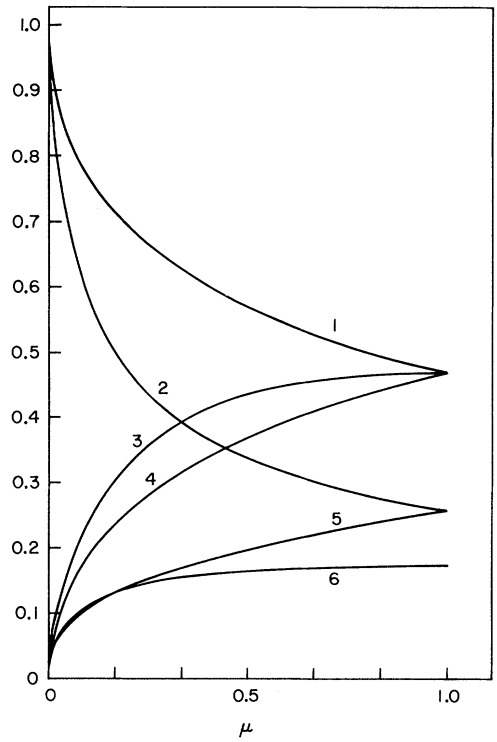

FIG. 2. This is the 1D↔2D analog of Fig. 1. Here $(K_\alpha a_\alpha)=(k,0)$ for curves 1 and 2, $(0,k)$ for curves 4 and 5, and (k,k) for curves 3 and 6. For curves 1, 3, and 4 $k=10^{-2}$, whereas for curves 2, 5, and 6 $k=\pi$. Here $v\to 0$ and $\mu=J_x/J_y$.

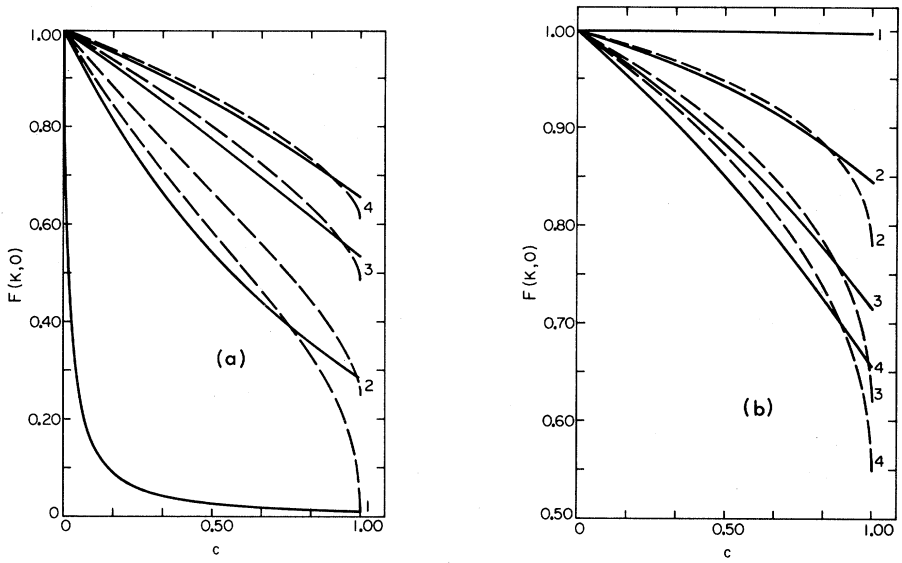

FIG. 3. To demonstrate 1D↔3D variation, the correlation factors f^0 and $F(\vec{K},0)$ are plotted as a function of the particle concentration. Again, the full curves refer to f^0 and the dashed ones to $F(\vec{K},0)$ with $\vec{K}$ at the zone edge. Relevant values of η for curves 1, 2, 3, and 4 are 10^{-4}, 10^{-1}, 0.5, and 1. For (a), the wave vector is parallel to the z axis, i.e., $(K_\alpha a_\alpha)=(0,0,k)$, whereas for (b) the wave vector is along the diagonal within the x-y plane, i.e., $(K_\alpha a_\alpha)=(k,k,0)$. Parameter $k=10^{-2}$ for the full curves and π for the dashed ones. Compare the full curves marked 1 in (a) and (b) with Eqs. (4.14b) and (4.18), respectively.

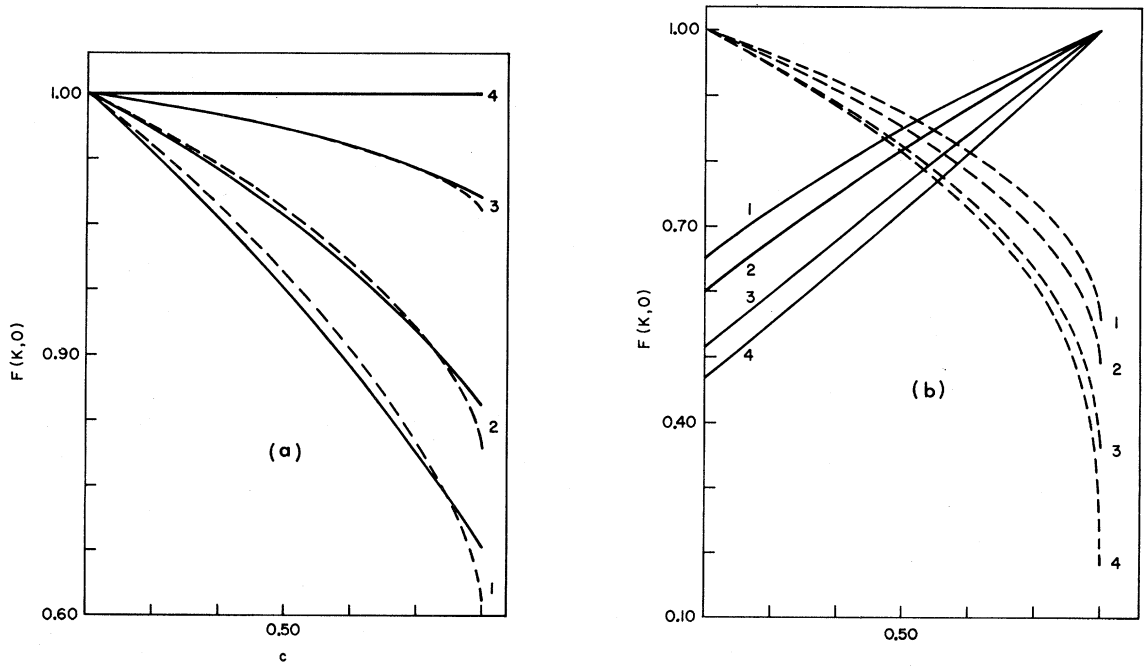

FIG. 4. Similar to Fig. 3 except that here the variation shown is for 2D↔3D. According, curves 1, 2, 3, and 4 refer to $\eta^{-1}=1$, 0.5, 10^{-1}, and 10^{-4}. Compare the solid curves marked 4 in (a) and (b) with Eqs. (4.14a) and (4.22), respectively. For convenience, the abscissa relating to the solid curves in (b) is v. For the dashed curves in (b) [as in Fig. 3(b)] the abscissa is c.

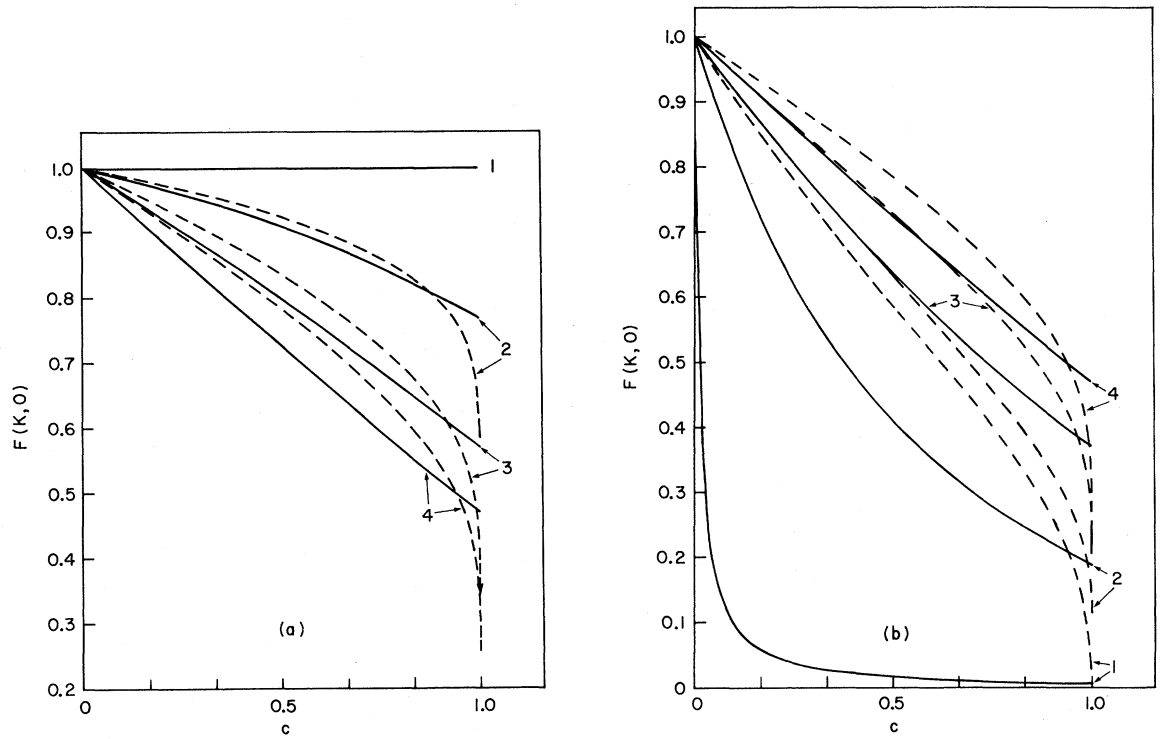

FIG. 5. Plot displays 1D↔2D variation in $F(\vec{K},0)$ as a function of concentration. Curves 1, 2, 3, and 4 refer to $\mu=10^{-4}$, 10^{-1}, 0.5, and 1 with (a) $(K_\alpha a_\alpha)=(k,0)$ and (b) $(K_\alpha a_\alpha)=(0,k)$. $k=10^{-2}$ for the solid curves and π for the dashed ones.

$(K_\alpha a_\alpha)=(0,\pi)$, $(\pi,0)$, and (π,π) are also included. Note that because of the inherent symmetry between the x and y directions only the case $1\geq\mu\geq 0$ need be studied.

While the $v\rightarrow 0$ limit is interesting, it is even more valuable to get a feel for how the change in concentration affects the various results. To this end in Figs. 3 and 4 we have shown the 1D↔3D and 2D↔3D characteristics as a function of the concentration. Here $F(\vec{K},0)$ is given for $\vec{K}$ along the linear chains, i.e., $(K_\alpha a_\alpha)=(k,0,0)$, as well as the diagonal in the x-y plane, i.e., $(K_\alpha a_\alpha)=(k,k,0)$. To obtain a convenient comparison between the diffusive and the large-$\vec{K}$ limits, results for both small k, i.e., $k=10^{-2}$, and for $k=\pi$, are provided.

These variations should be contrasted with those found during 1D↔2D passage. Accordingly, in Fig. 5 we have presented the latter. Again, the analytical results given above are corroborated. At the zone edge, the divergent slope for $v\rightarrow 0$ is noted in all dimensions.

The frequency dependence is analyzed in Figs. 6 and 7. For the sake of brevity, we consider only the small vacancy limit $v=0.01$ and show in Fig. 6 the incoherent response function for $(K_\alpha a_\alpha)=(0,0,\pi)$ for the nearly 1D case, i.e., $\eta=10^{-2}$. Such a choice of the wave vector $\vec{K}$ (namely, when it lies in the

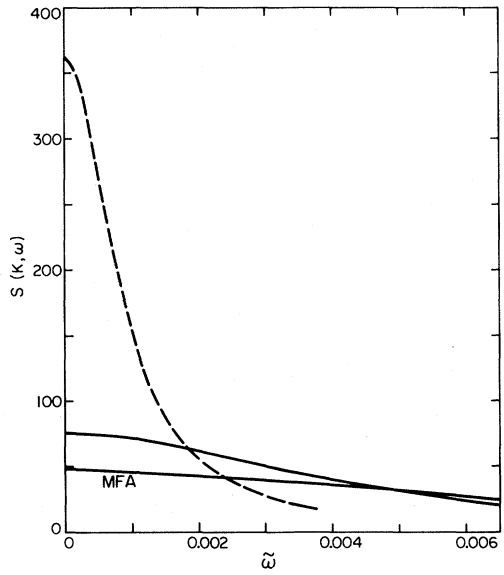

FIG. 6. For $v=0.01$ the incoherent scattering function $S(\vec{K},\omega)$ is plotted as a function of the normalized frequency $\tilde{\omega}=\omega/(6J_{||})$. Broken curve refers to the nearly 1D system with $\eta=0.01$, whereas the solid curve is for the isotropic 3D system (the simple cubic lattice) with $\eta=1$. Here $(K_\alpha a_\alpha)=(0,0,\pi)$. Solid curve marked MFA gives the corresponding mean-field-approximation results which happen to be the same for both these cases.

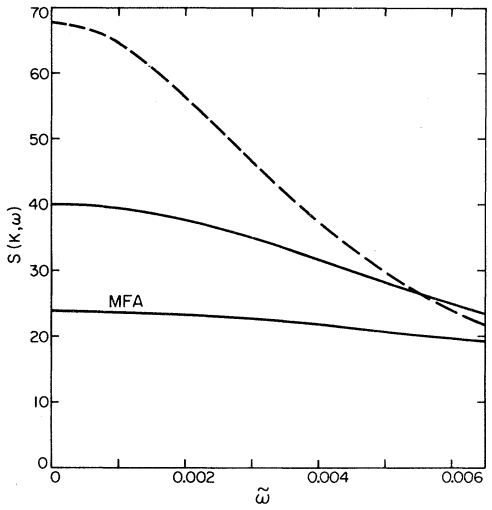

FIG. 7. $S(\vec{K},\omega)$ for $v=0.01$ is plotted as a function of the normalized frequency $\tilde{\omega}=\omega/(6J_1)$. Here the broken curve is for the nearly 2D case $\eta^{-1}=0.01$ whereas the solid curve is for the isotropic 3D system (the simple cubic lattice with $\eta=1$). Relevant wave vector is $(K_\alpha a_\alpha)=(\pi,\pi,0)$. Mean-field-approximation result, marked MFA, is the same for both these systems.

lower dimensionality) brings out the strongly correlated character of the nearly 1D system because then the MFA results for the 1D and the 3D systems are the same.

The corresponding, nearly 2D limit, i.e., $\eta^{-1}=10^{-2}$, is shown in Fig. 7. Again, to give a visual demonstration of the importance of correlations, we have chosen the wave vector to lie within the two dimensions, i.e., $(K_\alpha a_\alpha)=(\pi,\pi,0)$. This makes the MFA results for the given system as well as those for an isotropic 3D (simple cubic) system to be the same. We notice that while correlations are important in the 2D system (the actual, dotted curve, is more than $2\frac{1}{2}$ times as high at $\omega\to 0$ as the MFA), they are far less important here than in the nearly 1D limit (where the relative heights of the two corresponding curves were approximately eight to one).

ACKNOWLEDGMENTS

This work was started at the International Centre for Theoretical Physics (ICTP), Trieste, Italy. I am indebted to Professor E. Tossati and Professor A. Salam for hospitality at ICTP. The Monte Carlo work being carried out by Professor K. Binder and his associates Dr. R. Kutner and Dr. K. W. Kehr has provided special impetus for writing up this study. I am greatly indebted to Professor K. Binder, Professor R. J. Elliott, Dr. K. W. Kehr, and Dr. K. Schroeder for helpful discussions. Financial support from the National Science Foundation, NSF Grant No. DMR-80-13700, and from a Grant-in-aid of research from Temple University is gratefully acknowledged.

[1]For a recent review, see *Topics in Current Physics: Physics of Superionic Conductors,* edited by M. B. Salamon (Springer, Berlin, 1979).

[2]A comprehensive recent review and relevant bibliography is given by J. Völkl and G. Alefeld, in *Hydrogen in Metals,* Topics in Applied Physics, edited by G. Alefeld and J. Völkl (Springer, Berlin, 1978).

[3]See, for example, A. D. LeClaire, in *Physical Chemistry,* edited by H. Eyring, D. Henderson, and W. Jost (Academic, New York, 1970), Vol. 10.

[4]J. Bardeen and C. Herring, in *Imperfections in Nearly Perfect Crystals,* edited by W. Shockley (Wiley, New York, 1952).

[5]R. A. Tahir-Kheli and R. J. Elliott, Phys. Rev. B 27, 884 (1983).

[6]K. W. Kehr, R. Kutner, and K. Binder, Phys. Rev. B 23, 4931 (1981); R. Kutner and K. W. Kehr (unpublished); H. van Beijeren, K. W. Kehr, and R. Kutner (unpublished).

[7]R. A. Tahir-Kheli and R. J. Elliott, J. Phys. C 15, L445 (1982).

[8]P. M. Richards, Phys. Rev. B 16, 1393 (1977).

[9]P. A. Fedders, Phys. Rev. B 17, 40 (1978).

[10]S. Alexander and P. Pincus, Phys. Rev. B 18, 2011 (1978).

[11]U. V. Alpen, H. Schulz, G. H. Talat, and H. Bohm, Solid State Commun. 23, 911 (1977).

[12]W. L. Roth, F. Reidinger, and S. LaPlaca, in *Superionic Conductors,* edited by G. D. Mahan and W. L. Roth (Plenum, New York, 1976).

[13]P. A. Fedders and O. F. Sankey, Phys. Rev. B 18, 5938 (1978).

[14]R. D. Hogg, S. P. Vernon, and V. Jaccarino, Phys. Rev. Lett. 39, 481 (1977).

[15]S. P. Vernon, P. Thyamballi, R. D. Hogg, D. Hone, and V. Jaccarino, Phys. Rev. B 24, 3756 (1981).

[16]P. M. Richards, in Ref. 1.

[17]P. M. Richards, Phys. Rev. B 18, 6358 (1978).

[18]P. M. Richards, Phys. Rev. B 20, 2964 (1979).

[19]D. Brinkman, M. Mali, J. Roos, and E. Schweickert, Solid State Ionics 5, 433 (1981).

[20]P. M. Richards, Solid State Ionics 5, 429 (1981).

[21]K. Binder (private communication).